Journal of Hazardous Materials 197 (2011) 88–96

Contents lists available at SciVerse ScienceDirect

Journal of Hazardous Materials

journal homepage: www.elsevier.com/locate/jhazmat

Efficient degradation of organic dyes by $BiAg_xO_y$

Kai Yu[a,b], Shaogui Yang[a], Stephen A. Boyd[b], Hongzhe Chen[a], Cheng Sun[a,*]

[a] State Key Laboratory of Pollution Control and Resource Reuse, School of the Environment, Nanjing University, Nanjing 210093, PR China
[b] Department of Crop and Soil Sciences, Michigan State University, East Lansing, MI 48824, USA

ARTICLE INFO

Article history:
Received 3 May 2011
Received in revised form
14 September 2011
Accepted 15 September 2011
Available online 1 October 2011

Keywords:
Bismuth silver oxide
Oxidation
Dye degradation

ABSTRACT

A novel, simple and efficient approach for degrading organic dye, based on $BiAg_xO_y$ (bismuth silver oxide, BSO), is reported for the first time. The oxidative powder BSO was prepared by simple coprecipitation of $NaBiO_3{\cdot}2H_2O$ and $AgNO_3$. The technique was evaluated for the decolorization and oxidative decomposition of Rhodamine B (RhB). The results demonstrated that mixing BSO with an aqueous solution of RhB (20 mg/L) resulted in rapid decolorization (pseudo-first-order kinetic constant $k = 0.5594\ min^{-1}$) and formation of several small molecular weight products. Significant reduction in TOC (32% TOC removal in 10 min) also occurred via mineralization of RhB to CO_2/CO_3^{2-}. The reaction proceeds at ambient temperature and pressure, and requires no external energy sources or light. An advantage of the technique is that BSO can be used to degrade sequential additions of dye without significant fouling or loss of activity. The characterization of BSO and its corrosion products by XRD, FTIR, TEM, EDX and XPS revealed that Ag species were reduced to metallic silver and $NaBiO_3{\cdot}2H_2O$ was transformed into the $Bi_2O_2CO_3$ during the reaction process. Singlet oxygen ($^1O_2$) was identified as the major reactive species generated by BSO for the degradation of RhB and several other dyes. This novel approach could be used as a highly efficient and green technology for organic dye degradation.

1. Introduction

Organic dyes are extensively used for many applications including coloring fabrics, oil and fats, and as staining agents in bacteriological and histopathological applications [1]. Manufacture and use of organic dyes inevitably leads to their release into the environment. The inadvertent discharge or spillage of dyes into surface water may exert long term adverse effects on the aquatic environment. Such release of dyes can cause dramatic aesthetic pollution, and also pose a threat to ecosystem and human health due in part to the presence of commonly formed carcinogenic aromatic amine metabolites [2].

In contrast to the unsatisfactory utilization of direct biological treatment, flocculation, and activated carbon adsorption on dye wastewater treatment [3,4], chemical oxidation using ozonation, hydrogen peroxidation and permanganate oxidation, have been reported to be reasonably effective approaches to eliminate color and total organic carbon of dye wastewater [5–7]. Simple ozonation or hydrogen peroxidation are not efficient enough for the practical usage. Although permanganate oxidation can manifest a rapid degradation rate [7], considerable quantities of manganese salt are formed in water as the reaction proceeds, and this may thereby create a secondary pollutant. Considerable effort over decades has further improved and refined many advanced oxidation processes (AOPs). As such, AOPs are now recognized as promising technologies for water purification, and have gained considerable attention due to their rapid degradation rates and high oxidation capacities for decomposing organic pollutants. Although AOPs such as UV/H_2O_2, Fenton and sonocatalysis have been reported to efficiently degrade a variety of environmental pollutants including organic dyes [8–10], their application has been limited by the high cost of the continuous consumables needed for the degradation process, and the requirement for external auxiliary energy such as UV light or ultrasonic waves. Therefore, new technologies for the effective oxidation of dye pollutants, without the requirement of large amounts of numerous chemical reagents or powerful irradiation sources, are desirable. Furthermore, each new approach for concentrated dye removal, with its unique capabilities and limitations, adds to the arsenal of technologies for application to specific problems or sites of contamination. It has been recently demonstrated that perovskite-like metal oxide structure has oxygen storage capacity that can be successfully harnessed for environment remediation [11,12]. Moreover, this type of oxide is amenable to partial substitution of structural cations by other elements that may result in increased activity [12]. As such, these materials have the potential for extensive application in the treatment of dye contaminated wastewaters, including emergency situations involving dyes at high concentrations.

* Corresponding author. Tel.: +86 25 89680258; fax: +86 25 89680580.
E-mail address: envidean@nju.edu.cn (C. Sun).

0304-3894/$ – see front matter © 2011 Elsevier B.V. All rights reserved.
doi:10.1016/j.jhazmat.2011.09.056

The objective of this study was to develop and characterize a novel and effective material, based on the perovskite-type structure, for aquatic organic dye removal from water. In this study, we characterize the degradation activity of bismuth silver oxide (BSO), and elucidate the operative reaction mechanisms, using rhodamine B (RhB) as a model pollutant. This is the first study that utilizes a $NaBiO_3{\cdot}2H_2O$ based material to oxidize organic pollutants directly, i.e. not light-driven [13,14]. The proposed method can rapidly degrade aqueous phase organic dyes at room temperature and atmospheric pressure without the requirement of any auxiliary energy.

2. Materials and methods

2.1. Chemicals

$NaBiO_3{\cdot}2H_2O$ was purchased from LI-DE Offset Chemical Material Co. Ltd., China. Silver nitrate (≥99.8%) was produced by Sinopharm Chemical Reagent Co. Ltd., China. Rhodamine B (RhB, laser-grade) was obtained from Acros Chemical Company. 5,5-Dimethyl-1-pyrroline-N-oxide (DMPO) spin-trap reagent was supplied by Sigma Chemical Co. Other chemicals were of analytical grade and all were used as received. Deionized water supplied by a Milli-Q purification machine was used throughout this study.

2.2. BSO preparation and characterization

In a typical preparation, 0.1 g solid $AgNO_3$ was first dissolved in 100 mL of deionized water with stirring to form a homogeneous solution. Then 0.2 g $NaBiO_3{\cdot}2H_2O$ was added. Immediately, a black and maroon colored sediment formed which quickly became black and then remained unchanged. The whole reaction was completed in seconds. The resulting black colored solid was separated by centrifugation, and washed with deionized water to eliminate the possibly absorbed cations.

The purity and crystallinity of the BSO formed as described above were characterized by powder X-ray diffraction (XRD) using a Shimadzu diffractometer (LabX XRD-6000). Fourier transform infrared (FTIR) spectroscopy spectra were obtained with a NICOLET NEXUS 870 spectrometer. An ESCALAB 250 spectrometer (Thermo Fisher Scientific Inc.) with monochromatized Al Kα radiation was used for the X-ray photoelectron spectroscopy (XPS) analyses. Transmission electron microscopy (TEM) (JEOL JEM-200CX) was used to investigate the grain size and morphology of the sample particles. The elemental distribution of the sample was examined by energy dispersive X-ray (EDX) spectroscopy (HORIBA EX-250). Electron spin resonance (ESR) signals of radicals spin-trapped by DMPO were recorded on a Brucker EMX 10/12 spectrometer with a TM110 cavity for emittance exchange.

2.3. Degradation experiment

An evaluation of the BSO based treatment method was carried out by measuring the degradation of RhB in the aqueous phase. A 150 mL conical flask was used as a reactor which was wrapped in aluminum foil to avoid any effects of light. The prepared BSO was added to 100 mL RhB solution (20 mg/L) and stirred at a constant speed throughout the reaction process to ensure continuous contact between the solution and BSO. A sequential RhB degradation experiment was conducted to investigate BSO durability and its potential for corrosion resistance during degradation of RhB dye. A 100 mL RhB solution (25 mg/L) was reacted with BSO formed from 0.2 g $NaBiO_3{\cdot}2H_2O$ and 0.1 g $AgNO_3$. After the solution was decolorized, a certain amount of RhB stock (20 g/L) was added into the residual BSO slurry to raise the initial RhB concentration back to 25 mg/L. This sequence was repeated for a total of 16 cycles.

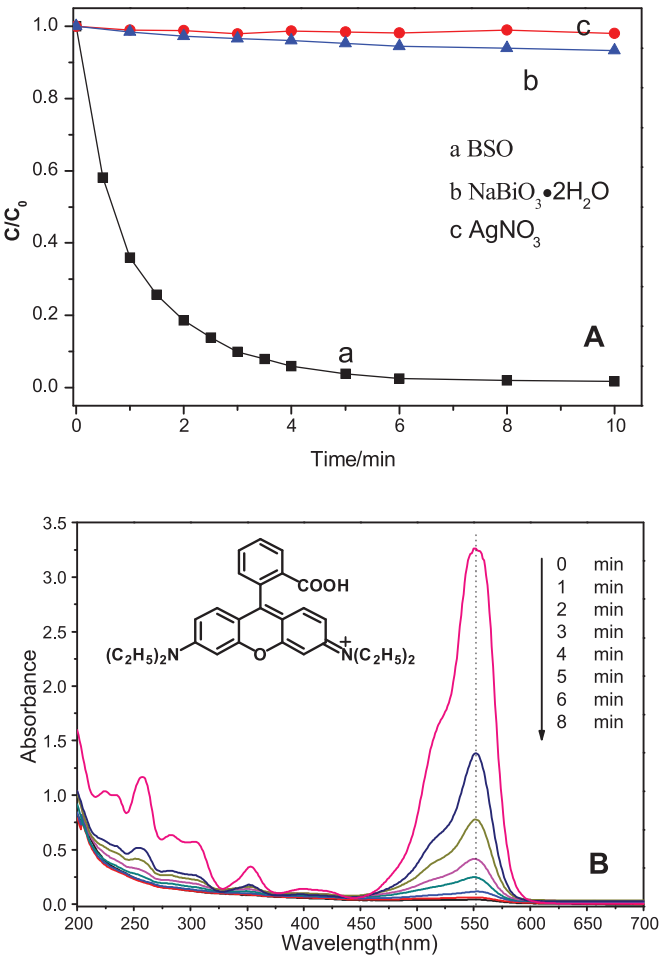

Fig. 1. (A) Time evolution of 100 mL RhB (20 mg/L) solution (a) with a certain amount of BSO formed from 0.2 g $NaBiO_3{\cdot}2H_2O$ and 0.1 g $AgNO_3$, (b) with 0.2 g $NaBiO_3{\cdot}2H_2O$ and (c) with 0.1 g $AgNO_3$. (B) UV–vis spectral changes corresponding to curve (a).

At given intervals, appropriate amounts of suspension were taken out and filtered before analysis. The concentration of RhB was measured by a Shimadzu UV-2450 spectrophotometer set at a absorbance maximum of 553 nm. Total organic carbon (TOC) was measured by a Shimadzu TOC-5000A. The GC/MS analyses were carried out on a Thermo Finnigan Trace gas chromatography interfaced with a Polaris Q ion trap mass spectrometer (Thermo, Finnigen, USA). The pre-treatment process for the GC/MS was conducted as reported in our previous study [13].

3. Results and discussion

3.1. RhB degradation

Rhodamine B, an extensively used commercial dye, was chosen as the model dye pollutant to evaluate the oxidative degradation ability of BSO. Reactions utilizing BSO were performed at room temperature and atmospheric pressure by simply stirring the BSO reagent with the dye solution. Fig. 1A shows representative data for the decomposition of RhB in water. In the control experiment utilizing $AgNO_3$ but lacking BSO, the amount of RhB in solution remained constant, i.e. there was no dye degradation. Similarly, in another control experiment with $NaBiO_3{\cdot}2H_2O$ only, a slight decrease in RhB concentration was observed which could be attributed to surface adsorption. Although both chemicals have been reported to possess photocatalytic activity and oxidative ability under certain conditions [14,15], RhB was not significantly decomposed by either under ambient conditions used in our experiment. In contrast, RhB

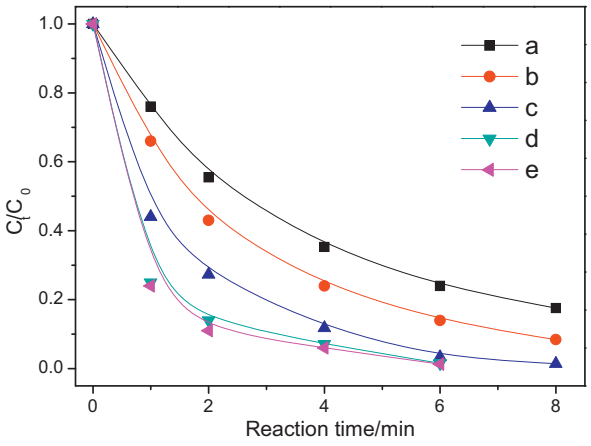

Fig. 2. Effect of BSO dosage on the degradation of RhB solution (25 mg/L). (a) 0.1 g $NaBiO_3{\cdot}2H_2O$ and 0.05 g $AgNO_3$ based BSO, (b) 0.15 g $NaBiO_3{\cdot}2H_2O$ and 0.075 g $AgNO_3$ based BSO, (c) 0.2 g $NaBiO_3{\cdot}2H_2O$ and 0.1 g $AgNO_3$ based BSO, (d) 0.25 g $NaBiO_3{\cdot}2H_2O$ and 0.125 g $AgNO_3$ based BSO and (e) 0.3 g $NaBiO_3{\cdot}2H_2O$ and 0.15 g $AgNO_3$ based BSO.

underwent rapid and extensive decomposition in the presence of the prepared BSO. More than 98.3% of the dye (4.5×10^{-3} mmol) was eliminated in 10 min by BSO (0.63 mmol of Bi and 0.37 mmol of Ag) with a pseudo-first-order kinetic constant $k = 0.5594\ min^{-1}$. A rapid decrease of the characteristic RhB absorption peak at 553 nm was observed, with concomitant reductions in absorption peaks at 258, 302 and 358 nm which correspond to the π–π^* transitions in the extensively conjugated double bond system of the aromatic ring structure of RhB (Fig. 1B). The UV–vis spectral changes demonstrated the facile cleavage of the conjugated chromophore. In addition to RhB, other dye solution at different concentration such as 100 mg/L of azure I, 50 mg/L of crystal violet, 100 mg/L of malachite green, 200 mg/L of safranin T and 150 mg/L of alizarin red were also found to be rapidly degraded (>90%) by BSO under the same reaction conditions in less than 9, 4, 5, 11 and 12 min, respectively. Due to the different property of these different subjects, the reaction time required for dyes elimination (>90%) varied. The results shown that not only triarylmethane family dye (rhodamine B, crystal violet and malachite green) but also safranin (safranin T), thiazin (azure B), anthraquinone (alizarin red) family dyes suffered severe degradation in the presence of BSO, indicating BSO is extensively effectual for organic dye wastewater remediation.

3.2. BSO dosage effect

The kinetic study to evaluate the effect of BSO dosage on RhB degradation is shown in Fig. 2. The decolorization rate of the RhB solution (25 mg/L) increased with increasing initial BSO concentration. Using the various BSO dosages i.e. 0.1, 0.15, 0.2 and 0.25 g ($NaBiO_3{\cdot}2H_2O$ based BSO), the pseudo first order rate constants for decolorization were calculated, which increased from 0.23 to 0.34 to 0.54 to 0.72 min^{-1}, respectively. As a heterogeneous reaction, when the BSO particle dosage is increased, the probability of reaction between dye molecules and BSO is expected, a priori, to increase, leading to an enhancement in the decolorization rate, as observed. Subsequent increase in BSO dosage beyond this level (i.e. >0.25 g $NaBiO_3{\cdot}2H_2O$ based BSO) resulted in marginal increases in the decomposition rates; the rate constant observed for reactions with 0.25 g and 0.3 g ($NaBiO_3{\cdot}2H_2O$ based BSO) were 0.72 and 0.76 min^{-1}, respectively. At these two BSO concentrations the RhB concentration (25 mg/L) presumably became the rate limiting parameter. Rate data from the present experiment, in which BSO is formed from 0.2 g $NaBiO_3{\cdot}2H_2O$ and 0.1 g $AgNO_3$ and the initial concentration of RHB was 25 mg/L, provides a starting point for optimizing the materials and operating costs of this new technology.

Table 1
Various RhB degradation intermediates identified by GC/MS.

Product	R_t (min)	M_w	Formula	Structure
1	14.07	62	$C_2H_6O_2$	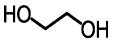
2	15.01	100	$C_6H_{12}O$	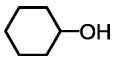
3	17.42	102	$C_5H_{10}O_2$	
4	19.82	90	$C_3H_6O_3$	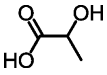
5	35.29	118	$C_6H_{14}O_2$	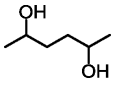
6	37.46	122	$C_7H_6O_2$	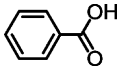
7	39.16	106	$C_4H_{10}O_3$	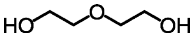
8	43.83	92	$C_3H_8O_3$	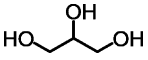
9	46.03	110	$C_6H_6O_2$	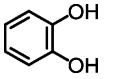
10	51.21	116	$C_4H_4O_4$	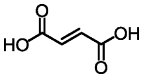
11	54.95	110	$C_6H_6O_2$	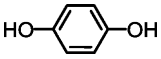
12	57.58	146	$C_6H_6O_2$	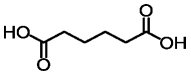

3.3. RhB mineralization and intermediates

Changes in total organic carbon (TOC) content indicate the degree to which an organic substrate is mineralized to CO_2 (or CO_3^{2-}) during the degradation process. The rapid removal of TOC is desired in practical application for it is a common water quality criterion, and demonstrates extensive decomposition of the parent compound. In the present study, simply stirring the RhB solution with BSO, absent of any auxiliary energy resulted in a significant reduction in TOC from 16.24 mg/L to 11.00 mg/L (32% reduction) in only 10 min.

Destruction of the conjugated chromophore structure was confirmed by GC/MS. Several small molecular weight organic compounds were extracted and identified as degradation intermediates by mass spectroscopy, utilizing the commercial library (NIST2) for structural assignments (Table 1). Among the twelve degradation products identified, the most commonly found structures were substituted benzenes and small molecular weight alcohols. The presence of these compounds in the reaction product mixture provides clear evidence that cleavage of the conjugated xanthene structure of RhB occurred, followed by further degradation to produce small molecular weight hydroxylated products. The significant reduction in TOC suggests the formation of volatile organic compounds among the reaction intermediates, and possibly CO_2 (or CO_3^{2-}).

3.4. Material durability

For the practical treatment of pollutants, it is desirable that the central reagent, BSO, not be readily fouled by the primary

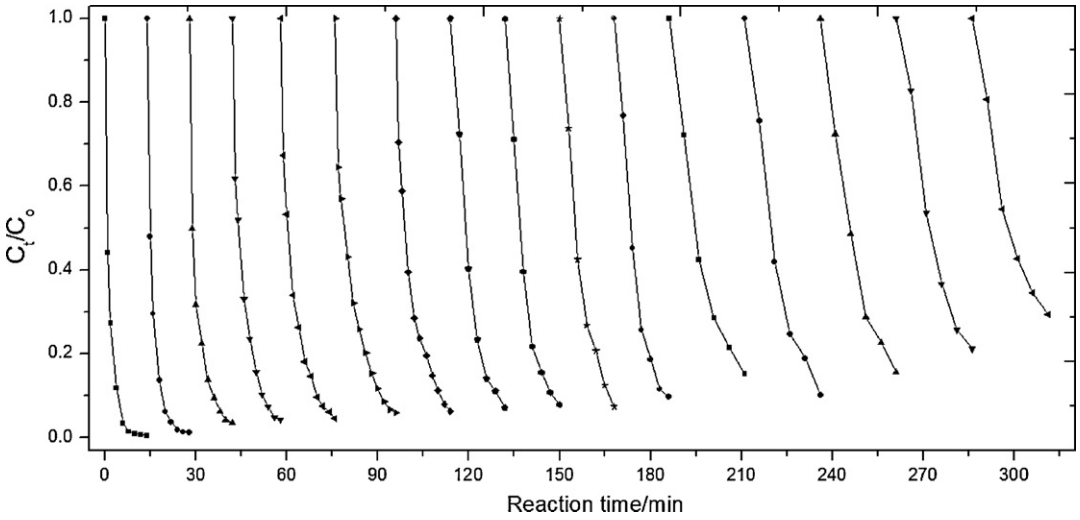

Fig. 3. Concentration decrease of RhB (initial 25 mg/L in each cycle) as a function of cyclic reaction time. BSO subjected to 16 sequential addition of RhB was formed from 0.2 g $NaBiO_3{\cdot}2H_2O$ and 0.1 g $AgNO_3$.

contaminant (e.g. RhB) or its degradation products during usage. In order to evaluate the potential deactivation of BSO, the same BSO particles were subjected to several sequential RhB additions (Fig. 3). It is evident that BSO (formed from 0.63 mmol of Bi and 0.37 mmol of Ag) remains reactive under such experimental conditions; RhB contained in 25 mg/L solution was completely eliminated or substantially reduced after each of 16 (0.09 mmol RhB total) sequential additions which occurred over a total time of approximately 5 h. In the first cycle, RhB degradation was completed within <15 min, which was the shortest time required to completely degrade the RhB in the cyclic reaction. The time required to remove subsequent RhB additions from solution by reaction with the residual BSO particles gradually lengthened during the 16 sequential additions of RhB. For the final (16th) addition, because of the activity decrease of the reused BSO 71% decolorization and 14% TOC removal of added RhB was achieved in 25 min. The final degradation products were mostly the same as those determined after the first run (Table 1), indicating that these intermediates are not easily subjected to further degradation in the presence of BSO generated active species (see discussion below). During the last cycle, the BSO activity had obviously decreased compared with freshly prepared BSO, but it could still effectively decolorize RhB, showing that it was still functional. It seems reasonable that BSO would continue to be active in degrading more RhB, albeit to a lesser extent, if the 17th cycle was executed. We selected 16 cycles to show that the BSO was not easily fouled, or rendered inactive, after its initial exposure to RhB, rather that it can be exposed to repeated dye additions without being prematurely deactivated. The final reaction solution was centrifuged and analyzed for Ag and Bi by atomic absorption. Both Ag and Bi were present at only trace quantities indicating an insignificant release of these metal ions into solution during the degradation process. In principle, the solid residue material could be filtered and the noble metal i.e. metallic Ag (discussed below), could plausibly be regenerated for further use. Taken together, these attributes suggest the practical utility of BSO for dye removal, with minimal ancillary adverse effects to the aquatic environment.

3.5. BSO characterizations

In the sequential dye degradation experiments, the solids were recovered from the dye reaction suspension, washed with water, and then ultrasonic ethanol washing was repeated five times to remove any adsorbed organics. In all instances, the recovered solids (BSO and BSO after reaction with dye) were freeze-dried prior to further analysis. For comparison, $AgBiO_3$ was synthesized according to published procedures [16].

3.5.1. XRD analysis

For the purpose of examining changes in the crystalline structure of BSO associated with the RhB dye degradation reaction, the residual powders used in the cyclic experiments were separated and analyzed by X-ray powder diffraction. Fig. 4 shows the XRD patterns of six different BSO samples and two standard materials. The freshly prepared sample shows only one strong distinct diffraction peak at $2\theta = 32^\circ$ which matches the strongest and most characteristic peak of $NaBiO_3{\cdot}2H_2O$ in the perovskite-like structure [13,17]. Considering the similarity between the BSO synthetic procedure used here, and the standard $AgBiO_3$ synthesis [16], it is plausible that the prepared BSO sample closely resembles $AgBiO_3$ in the perovskite-like structure, hence manifesting the $2\theta = 32^\circ$ peak. After three successive addition of RhB (i.e. 3 cycles), the $2\theta = 32^\circ$ peak intensity decreased slightly indicating some transformation of the perovskite structure. In addition, several new peaks appeared in the XRD pattern for the residual BSO, most of which coincide

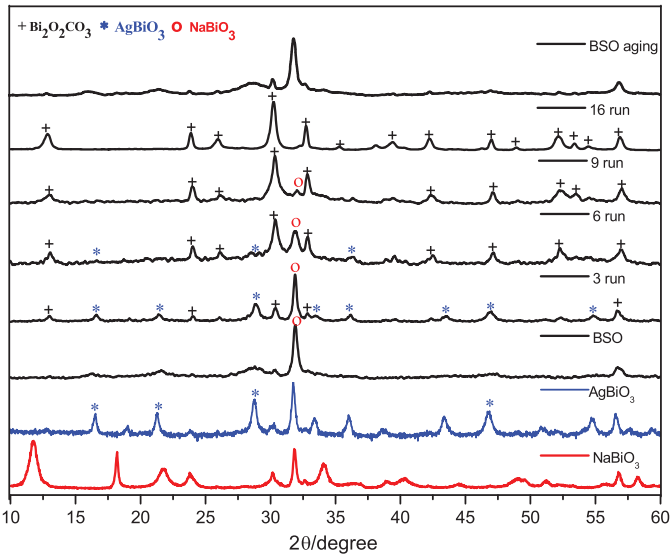

Fig. 4. XRD patterns of two standard materials, viz. $NaBiO_3{\cdot}2H_2O$ and $AgBiO_3$, and BSO after 3, 6, 9 and 16 sequential exposures of RhB solutions, and BSO aged for 5 h.

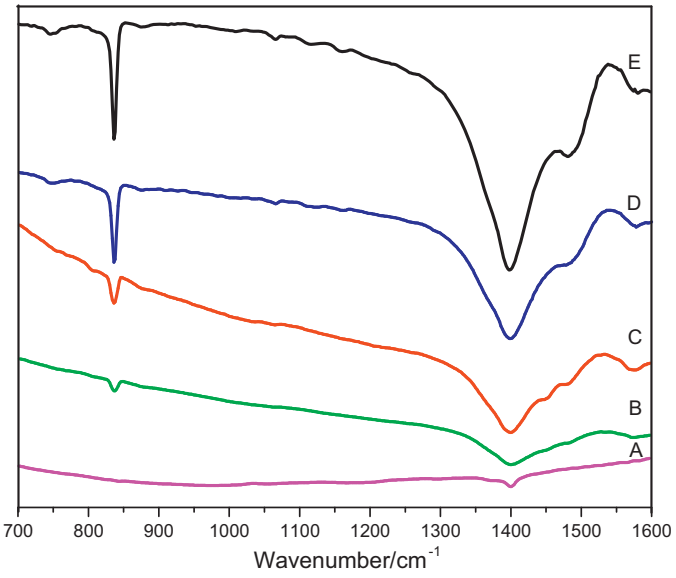

Fig. 5. FTIR spectra of residual BSO powder after various cycles of sequential RhB addition (A) freshly prepared sample, (B) BSO after 3 cycles, (C) BSO after 6 cycles, (D) BSO after 9 cycles and (E) BSO after 9 cycles of sequential RhB addition.

with the standard $AgBiO_3$ pattern, including peaks at $2\theta = 16.5^\circ$, 21.3°, 28.7°, 33.4°, 36°, 43.4°, 46.3° and 54.7°. These new peaks indicate that $AgBiO_3$ gradually became more crystalline during the first three successive additions of RhB. Some other small peaks at $2\theta = 12.9^\circ$, 23.9°, 30.2° and 32.7° in the same spectrum may represent the formation of small amounts of $Bi_2O_2CO_3$. The XRD pattern obtained for residual BSO after 6 cycles of RhB addition showed that the characteristics perovskite peak at $2\theta = 32^\circ$ decreased further, and the emergence of other peaks characteristic of $Bi_2O_2CO_3$ at $2\theta = 25.94^\circ$, 42.24°, 46.95° and 52.14°. The 9-cycle sample displayed a similar XRD pattern to that of the previous (6-cycle) sample, but with increased intensity for all peaks assigned to $Bi_2O_2CO_3$, and a much smaller peak at $2\theta = 32^\circ$. In the samples after 9 and 16 cycles of RhB addition the $AgBiO_3$ peaks had essentially disappeared suggesting that the $AgBiO_3$ structure had largely decomposed and been replaced by $Bi_2O_2CO_3$ which appeared to be the major crystalline phase present. After the 16th cycle, the sample presented a XRD pattern identical to that of $Bi_2O_2CO_3$ (JCPDS 411488), and no other XRD peaks were observed. Thus, the prepared BSO had largely changed to $Bi_2O_2CO_3$ structure after 16 exposures to the RhB solution. To further elucidate the formation and stability of BSO, an aging experiment was conducted. After stirring BSO in water for more than 5 h, no significant changes were observed in the XRD pattern indicating that BSO prepared in this study was stable in water, and the observed changes occurred as a result of its reaction with RhB.

3.5.2. FTIR analysis

The FTIR analysis was performed in the 1600–700 cm^{-1} frequency range on powders taken from the BSO–RhB reaction suspensions (Fig. 5). Except for the freshly prepared BSO, all samples presented an intense broad band centered at 1398 cm^{-1}, and a sharp medium absorption band at 845 cm^{-1}. The 1398 cm^{-1} band is attributed to the stretching vibration of carbonate that resides in the narrow crystal lattice of $Bi_2O_2CO_3$, and the 845 cm^{-1} band is assigned to the ν_2 mode of carbonate, as it is characteristic of metal carbonates [18]. Clearly, both of the FTIR peaks support the formation and existence of $Bi_2O_2CO_3$. It was also noted that the two aforementioned bands increased in intensity as the number of cycle increased, consistent with the scenario that the prepared BSO was gradually reduced to $Bi_2O_2CO_3$ during successive cycles of RhB degradation, consistent with the XRD results (Fig. 4). Furthermore, the formation of $Bi_2O_2CO_3$ from BSO suggests the reaction creates a carbonate-existing environment [19] which provides a rationale for the observed decrease in TOC in the dye suspension. Additionally, it demonstrates the extensive degradation, and ultimately mineralization (i.e. CO_2 or CO_3^{2-}), of RhB via its reaction with BSO.

3.5.3. XPS analysis

XPS was used to further examine the details of BSO sample changes that accompanied the sequential RhB additions/reactions. The profiles corresponding to the elements Ag, O and Bi (Fig. 6) give information regarding the nature of the three species present at the surface of the samples where most catalytic and oxidative reactions are known to occur. The data were background subtracted according to Shirley's method [20] and fitted with different sets of peak parameters related to different species within the samples.

In the full XPS spectrum, the atomic ratio of Ag:Bi was about 1:1.1, whereas the ratio was 1:1.7 when the sample was analyzed by EDX. Considering XPS is highly surface-sensitive [21], the lower ratio indicates that silver tends to segregate at particle surfaces rather than be uniformly distributed throughout the bulk powder. The normalized Ag $3d_{5/2}$-XPS signals are given in Fig. 6A. The binding energy of the $3d_{5/2}$ level is equal to 368.1 eV for metallic Ag, and 367.8 eV for Ag (I); the less common Ag $3d_{5/2}$ peak at 367.3 eV indicates the presence of Ag (III) [22]. The binding energy of Ag in the freshly prepared BSO sample was 367.3 eV, demonstrating that Ag (in the prepared BSO) was in the trivalent state before dye degradation commenced. This agrees with the XRD analysis which provided evidence that Ag, in the initially formed BSO, was incorporated within the perovskite lattice in which it exists as Ag (III). After the three initial RhB degradation cycles, Ag (I) species formed as evidenced by the emergence of its characteristic binding energy at 367.8 eV [23]; the Ag (I) accounted for approximately 25% of the total silver species in the sample (based on the peak area at 367.8 eV). After the second set of three RhB degradation cycles (six total), the proportion of total silver as Ag (I) sharply increased to 80% based on the area of the peak at 367.8 eV, accompanied by the continuous break down of the perovskite structure. In the particle region sampled by XPS, the Ag (III) initially present in BSO had almost completely disappeared after nine cycles of sequential dye additions as indicated by the diminution of the peak at 367.3 eV. At this stage, metallic Ag had formed as indicated by the emergence of a peak at 368.1 eV. At the end of the 16 repetitions, XPS spectral data indicated that virtually all silver species existed as metallic Ag, which likely coated the exterior of the residual particles.

The XPS spectra of the O 1s transition are shown in Fig. 6B. The binding energy of O 1s electrons in oxygen bonded to metal cations has been regarded as one of the most informative parameters with respect to the structure of the oxide [23]. In the present samples, the O 1s peak can be deconvoluted into three distinguishable peaks with binding energies of 529.5, 530.8 and 532.5 eV. According to the simple classification proposed by Dimitrov and Komatsu [24], the O 1s feature at 529.5 eV is characteristic of lattice oxygen. The relative intensity of the peak at 529.5 eV weakened after several sequences of dye addition (Fig. 6B), indicating that oxygen initially present in the crystalline lattice diminished during the degradation process. This loss logically stems from transformation of the perovskite lattice to $Bi_2O_2CO_3$ (as indicated by XRD results, see above) as the added dye undergoes oxidative decomposition. The peak at 530.8 eV indicates the presence of weakly bound oxygen species, commonly characterized as "active and movable oxygen" or "chemisorbed oxygen" [25]. The change in the oxygen signal as

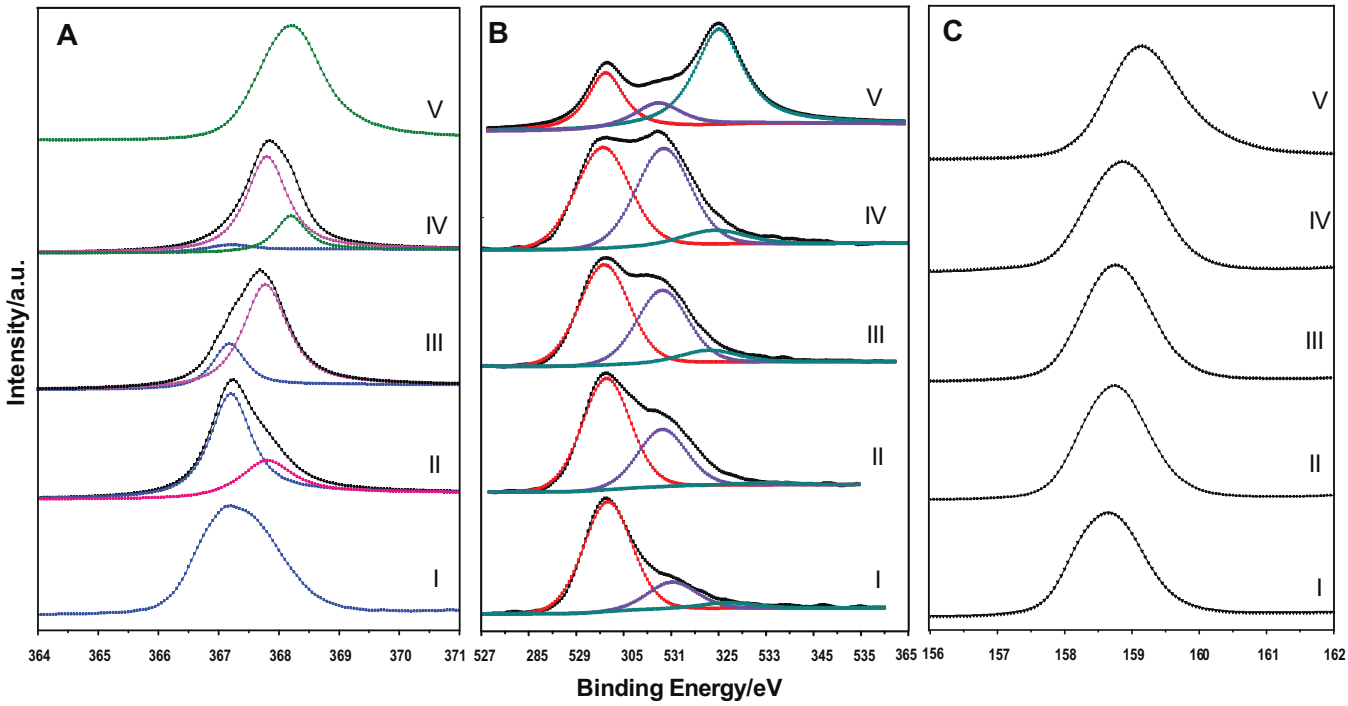

Fig. 6. XPS spectra of residual BSO powder after various cycles of sequential RhB addition. Ag $3d_{5/2}$ transition (A), O 1s transition (B), and Bi $4f_{7/2}$ transition (C) for differently recycled samples: (I) fresh sample, (II) after 3 cycles, (III) after 6 cycles, (IV) after 9 cycles, (V) after 16 cycles of RhB addition.

a function of the number sequential dye additions showed that the "active" oxygen (530.8 eV) reached a maximum value after nine repetitive degradation cycles, at which point it accounted for > 50% of the total oxygen species. After 16 cycles of dye addition, the "active" oxygen species declined to less than ~15% of the total oxygen. Furthermore, the last deconvoluted binding energy at 532.5 eV, attributed by adsorbed oxygen [26], emerged which most likely corresponds to oxygen incorporated in carbonate of $Bi_2O_2CO_3$, consistent with the results described above. Its change temporally also agrees well with the gradual emergence of $Bi_2O_2CO_3$ observed by XRD and FTIR.

As shown in Fig. 6C, it appeared that the Bi $4f_{7/2}$ peaks shifted to higher values (i.e. from 158.7 to 159.1 eV) with increasing the number of dye additions. Nevertheless, this increase does not indicate

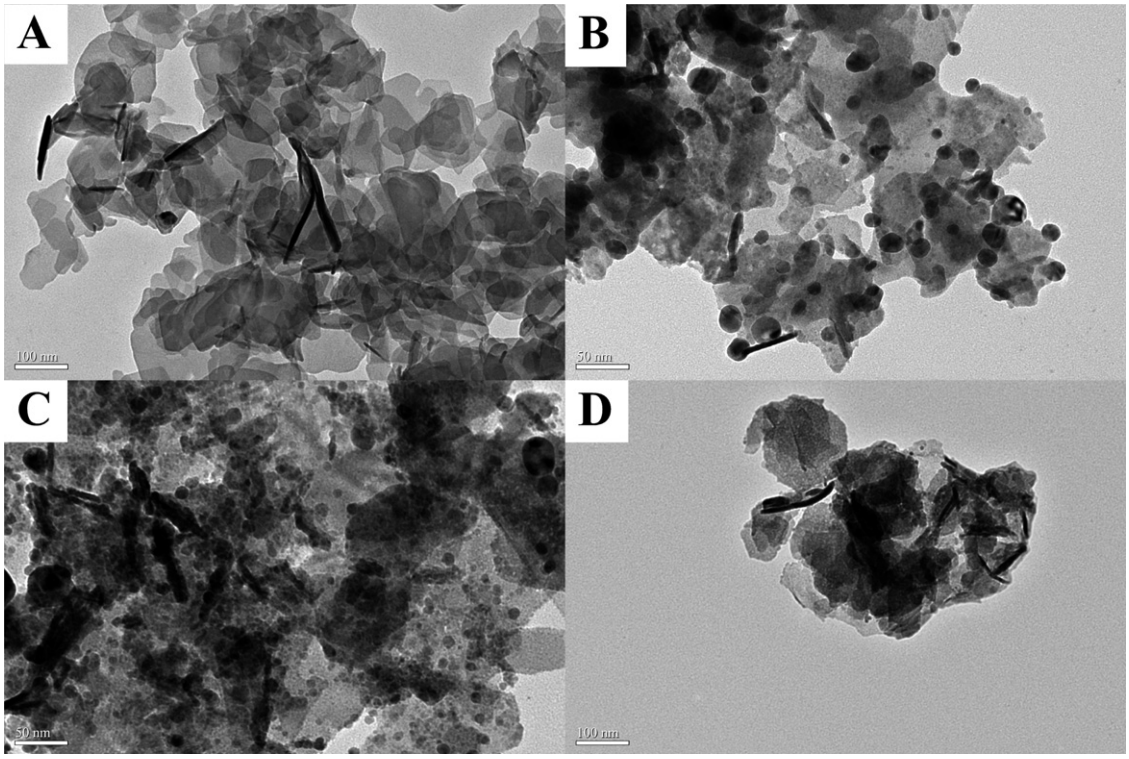

Fig. 7. TEM micrographs of $NaBiO_3 \cdot 2H_2O$ (A), freshly prepared BSO (B) and BSO after 9 (C) and 16 (D) sequential additions of RhB.

an oxidation of bismuth, especially not for the bulk bismuth. In fact, the only plausible change is that oxidized bismuth initially present in BSO was reduced during the RhB degradation, as indicated by XRD analysis. Considering the shallow detection depth of XPS, the anomalous Bi $4f_{7/2}$ electron behavior likely only exists on the surface of the sample and may be related to the formed reduced silver species which resides on the external surface of the sample particles, hence in close proximity to surface Bi. When Ag was first incorporated into the perovskite cell (replacing Na), the Ag–O bonds formed would simultaneously weaken the Bi–O bond. This may explain why the initially observed binding energy of Bi at 158.7 eV was lower than the characteristic 159.4 eV assigned to Bi in $NaBiO_3$. The continuous shift of the Bi signal to higher values could plausibly be related to the reduction of Ag (III). Accordingly, in concert with the reduction of silver, the electron density of the Ag–O bond shifted to oxygen thereby weakening of the Ag–O bond, which would concomitantly enhance the binding energy of bismuth via the Bi–O bond, as observed. Hence, the trends in the position of the Bi band in the XPS appear to be strongly influenced by the formation and location of metallic Ag at the particle surface which corresponds to the approximate sampling depth of XPS in our experiments.

3.5.4. TEM analysis

Typical morphologies of the samples obtained at different points during the reaction sequence were characterized by TEM (Fig. 7). The initially present $NaBiO_3{\cdot}2H_2O$ clearly exhibited a plate/flake shape with a size of about 100 nm (Fig. 7A). After reacting with $AgNO_3$, some darkened clusters with an average diameter of 20 nm were dispersed over the large parts of the flake, which are believed to be silver derivatives (Fig. 7B). While the number of RhB additions and degradation proceeded (through nine cycles), the silver clusters diminished in size to about 5 nm in diameter, and became more dense and uniformly distributed (Fig. 7C). This could be tentatively ascribed to the weakening total field strength [27] of Ag cation, caused by the progressive reduction from Ag (III)–O to Ag (I)–O. In the final samples (after 16 cycles of RhB addition) the silver clusters were irregularly shaped and difficult to image (Fig. 7D); the sample outline appeared diffuse compared to prior samples (Fig. 7A). In general, these observations seem consistent with initially oxidized silver species undergoing reduction to metallic Ag, which formed amorphous coatings on the particle exteriors, in accordance with the XPS results. The proposed corrosion process is also supported by observed color changes of the sample surface. As the repetitive dye additions progressed, the color of BSO gradually changed from pure black to brownish black, then to brown with some silvery white metallic luster on the exterior. The silvery luster was also present on the surface of the reaction solution, which is believed to be metallic silver that had separated from the particle. The visual observations are qualitatively consistent with a process proceeding from $AgBiO_3$ (black) [28] initially, to $Bi_2O_2CO_3$ (brownish yellow) and some Ag (silvery white) ultimately, which accompanied the sequential additions of RhB solutions.

3.6. Active oxygen species analysis

To further investigate the mechanistic function of BSO, three radical scavengers were employed to assess the contribution of various radical species to the oxidative decomposition of RhB. Tert-butyl alcohol has low affinity for particle surfaces in aqueous media, whereas it can react quickly with bulk •OH [29]. Hence, it was used as a diagnostic tool for dissociative hydroxyl radicals. Adding excess *t*-BuOH (30 mM) did not substantially change the decolorization rate of RhB indicating that bulk hydroxyl radicals do not take part in the degradation process (Fig. 8A). Potassium iodide is a scavenger

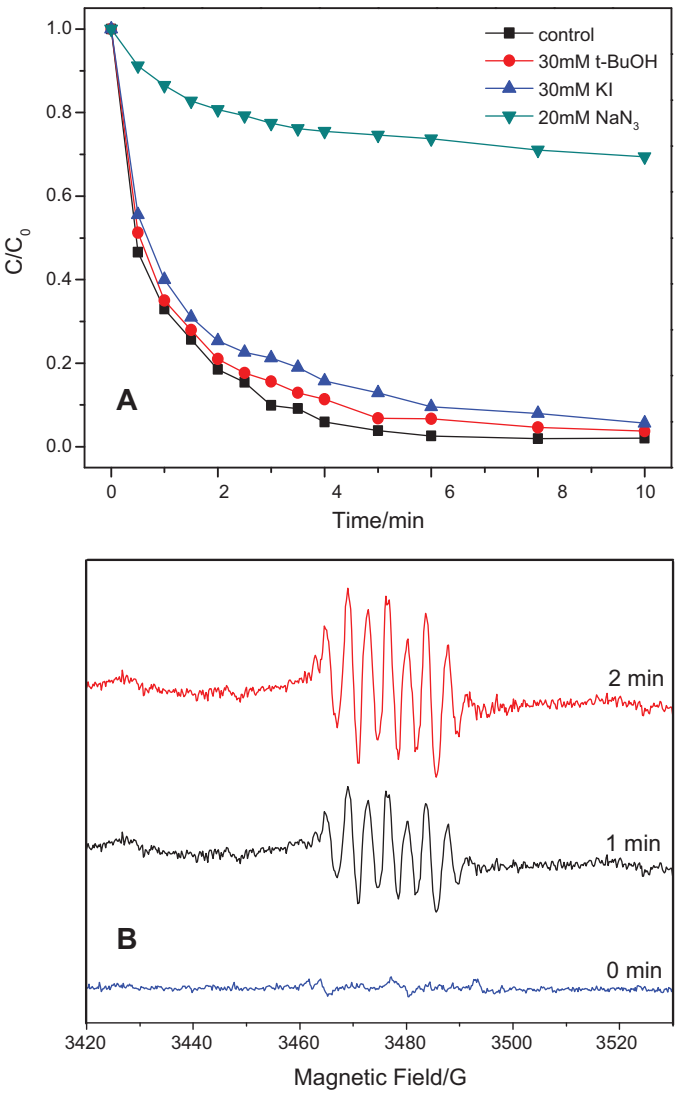

Fig. 8. (A) Effect of three radical scavengers, viz. tert-butyl alcohol (30 mM), KI (30 mM) and NaN_3 (20 mM) on degradation of 20 mg/L RhB mixed with BSO. (B) EPR spectra of DMPO spin-trapping reagent for singlet oxygen initially and after mixing with BSO dispersions in dark for 1 and 2 min. The characteristic 7-line spectrum of DMPO oxidized by singlet oxygen is observed in the presence of BSO.

that selectively quenches OH adsorbed on particle surfaces [30]. When 30 mM KI was added, no distinct changes were observed in BSO performance indicating that adsorbed hydroxyl radicals also do not play a major role in the decolorization process (Fig. 8A). However, in the presence of sodium azide (20 mM), a standard scavenger for singlet oxygen [31], the decolorization rate of RhB sharply decreased; only 30% of RhB was degraded after 10 min reaction time (Fig. 8A) compared to >98% reduction in its absence. This suggests that singlet oxygen is the central oxidant responsible for chromophore cleavage in RhB.

The EPR spectra of the DMPO-trapped $^1O_2$ were obtained. In the control experiment, only small background EPR signals were observed (Fig. 8B). The characteristic peaks of DMPO-OH and DMPO-OOH (in methanol media) adducts were not present, confirming the absence of these two common active oxygen species. Notably, after 1 min of stirring of BSO, the EPR spectrum exhibited seven lines (three longer and four shorter), corresponding to a derivative of DMPO oxidized by singlet oxygen, viz. 5,5-dimethyl-2-pyrrolidone-1-oxyl (DMPOX) [32]. The intensity of the peaks increased further with 2 min of stirring. These results strongly

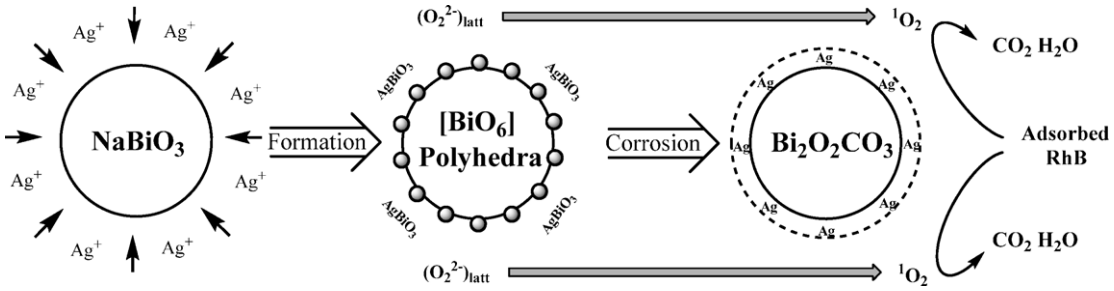

Fig. 9. Diagrammatic scheme for the formation of bismuth silver oxide (BSO) and its degradation of RhB dye via generation of singlet oxygen as the primary reactive species.

suggest that singlet oxygen is the sole active oxygen species in the degradation reaction of RhB via its reaction with BSO.

A control experiment was performed under dissolved oxygen free conditions to evaluate the possible role of dissolved oxygen in the degradation process. To better document of any changes associated with the absence of dissolved oxygen, the time required for complete decolorization of RhB (20 mg/L) under ambient conditions was prolonged to 30 min by reducing the dosage of BSO. When the entire BSO/RhB reaction was conducted under oxygen free environment with all other conditions unchanged, the reaction rate constant dropped by ~17%, suggesting that soluble oxygen molecules could facilitate the RhB degradation process as a minor source of active species.

3.7. Mechanism

On the basis of the complementary macroscopic and spectroscopic measurements described herein, the mechanistic function of the prepared BSO is tentatively proposed (Fig. 9). With the addition of $NaBiO_3{\cdot}2H_2O$ to the $AgNO_3$ solution, loss of Na from the perovskite lattice occurred accompanied by replacement with Ag. The combination of elemental, EDX, XRD and XPS analyses provides good evidence that silver was incorporated into the perovskite lattice by replacing sodium, especially at or near the particle surface, via the reaction [33]:

$$NaBiO_3{\cdot}2H_2O + AgNO_3 \rightarrow AgBiO_3 + NaNO_3 + 2H_2O \quad (1)$$

Because the radius of the Ag cation is larger than that of the Na cation, it is difficult for silver to fully permeate into the lattice. Thus, $AgBiO_3$ often forms slowly over time [13]. However, because the perovskite structure is sufficiently unstable, the loss of sodium cations (which are replaced by Ag cations) positioned between the networks of $[BiO_6]$ polyhedral in the original limonite phase is allowed [28]. As a result, the relatively strongly bonded crystal lattice oxygen transformed into relatively weakly bonded oxygen which released into solution where it transformed into active oxygen via reduction of Bi (V) [18]:

$$2Bi(V){-}O^{2-} \rightarrow 2Bi(IV){-}O^{-} \rightarrow Bi(IV){-}O_2{}^{2-}Bi(IV) \rightarrow Bi(IV){-}O_2{}^{-} + Bi(III) \rightarrow 2Bi(III) + O_2 \quad (2)$$

The singlet oxygen formed functioned as the central reactive species responsible for the degradation of RhB dye. Most commonly, singlet oxygen is generated by photosensitization of triplet molecular oxygen, or via several other chemical reactions, mostly involving hydrogen peroxide. It has also been reported that the aqueous decomposition of high valence metals such as potassium per chromate [34] without hydrogen peroxide can also contribute to $^1O_2$ formation. The "active" oxygen liberated by the reduction of Bi (V) was identified by XPS, and labeled as "chemisorbed oxygen". As discussed above, the ratio of active oxygen increased during the initial cycles of RhB additions, then decreased with subsequent cycles, whereas the lattice oxygen continuously decreased with increasing RhB additions. The EPR analysis indicated that singlet oxygen generated from lattice oxygen was the primary species responsible for the degradation of RhB. The observation that the incomplete, but not insignificant degree of mineralization of RhB does support the mechanistic interpretations, and identification of singlet oxygen as the primary active species. This is because singlet oxygen is not a strong active species, compared with hydroxyl radical as well known.

As Bi (V) was gradually reduced with successive cycles of RhB, the perovskite structure was destroyed and bismutite ($Bi_2O_2CO_3$) formed. This could be attributed to the generation of carbonate during the RhB decomposition. The carbonate species would be chemisorbed on the particle surface and saturate the oxygen defects [17]. Meanwhile, high valence silver species in proximity to the particle surface was reduced to metallic silver which covered the particles and plausibly enhanced the particle oxidizing power through the noble metal catalytic effect [33]. Hence, it is a complex process not just a pure oxidant involved in a simple oxidation reaction that can be directly compared with other typical oxidation reactions.

4. Conclusion

In summary, BSO provides a novel, facile and simple approach for organic dye degradation. This novel approach is efficient for decolorizing organic dyes in aqueous solution. The oxidative decomposition of dye results in the formation of smaller less toxic compounds, including CO_2 ($CO_3{}^{2-}$). This technology offers the practical advantages of relatively low operating costs, requiring less external energy input, and a very simple one-step synthesis to form the reactive BSO material, which is corrosion resistant to some extent. As such, BSO provides the basis for a very promising and practical environmental technology for the efficient treatment of dye effluent.

Acknowledgements

This work was supported by the National Natural Science Foundation of China (50938004 and 20737001) and Natural Science Foundation of Jiangsu Province (BK2009254).

References

[1] C.C. Chen, C.S. Lu, F.D. Mai, C.S. Weng, Photooxidative N-de-ethylation of anionic triarylmethane dye (sulfan blue) in titanium dioxide dispersions under UV irradiation, J. Hazard. Mater. 137 (2006) 1600–1607.
[2] L. Waldau, Dye industry – harmful and harmless substances, Kem. Tidskr. 91 (1979) 20–23.
[3] H. Xu, W.G. Xu, J.F. Wang, Degradation kinetics of azo dye reactive red SBE wastewater by complex ultraviolet and hydrogen peroxide process, Environ. Prog. Sustain. 30 (2011) 208–215.
[4] Y.M. Slokar, A.M. Le Marechal, Methods of decoloration of textile wastewaters, Dyes Pigments 37 (1998) 335–356.
[5] M.M. Hassan, C.J. Hawkyard, Ozonation of aqueous dyes and dyehouse effluent in a bubble-column reactor, J. Environ. Sci. Health 37 (2002) 1563–1579.

[6] J.S. Park, H. Choi, K.H. Ahn, The reaction mechanism of catalytic oxidation with hydrogen peroxide and ozone in aqueous solution, Water Sci. Technol. 47 (2003) 179–184.
[7] X.R. Xu, H.B. Li, W.H. Wang, J.D. Gu, Decolorization of dyes and textile wastewater by potassium permanganate, Chemosphere 59 (2004) 893–898.
[8] Y.G. Adewuyi, Sonochemistry in environmental remediation. 1. Combinative and hybrid sonophotochemical oxidation processes for the treatment of pollutants in water, Environ. Sci. Technol. 39 (2005) 3409–3420.
[9] C. Galindo, P. Jacques, A. Kalt, Photodegradation of the aminoazobenzene acid orange 52 by three advanced oxidation processes: UV/H_2O_2 UV/TiO_2 and VIS/TiO_2 – comparative mechanistic and kinetic investigations, J. Photochem. Photobiol. B 130 (2000) 35–47.
[10] W.G. Kuo, Decolorizing dye waste-water with fenton reagent, Water. Res. 26 (1992) 881–886.
[11] Y. Teraoka, K. Kanada, S. Kagawa, Synthesis of La–K–Mn–O perovskite-type oxides and their catalytic property for simultaneous removal of NO_x and diesel soot particulates, Appl. Catal. B 34 (2001) 73–78.
[12] B. Bialobok, J. Trawczynski, T. Rzadki, W. Mista, M. Zawadzki, Catalytic combustion of soot over alkali doped $SrTiO_3$, Catal. Today 119 (2007) 278–285.
[13] K. Yu, S.G. Yang, H. He, C. Sun, C.G. Gu, Y.M. Ju, Visible light-driven photocatalytic degradation of rhodamine B over $NaBiO_3$: pathways and mechanism, J. Phys. Chem. A 133 (2009) 10024–10032.
[14] T. Kako, Z.G. Zou, M. Katagiri, J.H. Ye, Decomposition of organic compounds over $NaBiO_3$ under visible light irradiation, Chem. Mater. 19 (2007) 198–202.
[15] T.X. Liu, X.Z. Li, F.B. Li, $AgNO_3$-induced photocatalytic degradation of odorous methyl mercaptan in gaseous phase: mechanism of chemisorption and photocatalytic reaction, Environ. Sci. Technol. 42 (2008) 4540–4545.
[16] N. Kumada, N. Kinomura, A. Sleight, Neutron powder diffraction refinement of ilmenite-type bismuth oxides: $ABiO_3$ (A = Na, Ag), Mater. Res. Bull. 35 (2000) 2397–2402.
[17] P. Feng, C.L. Chen, Y. Hao, H.J. Wang, Y. Jian, Preparation of $Na_xBa_yBiO_3$ nH_2O and their photooxidation characteristic under visible-light irradiation, Mater. Chem. Phys. 116 (2009) 294–299.
[18] D. Barreca, F. Morazzoni, G.A. Rizzi, R. Scotti, E. Tondello, Molecular oxygen interaction with Bi_2O_3: a spectroscopic and spectromagnetic investigation, Phys. Chem. Chem. Phys. 3 (2001) 1743–1749.
[19] C.C. Huang, K.Z. Fung, Effect of water/water vapor on microstructure and phase stability of $(Y_{0.25}Bi_{0.75})_2O_3$ solid electrolytes, J. Mater. Res. 18 (2003) 2624–2632.
[20] D.A. Shirley, High-resolution X-ray photoemission spectrum of the valence bands of gold, Phys. Rev. B 5 (1972) 4709–4714.
[21] H.J. Zhang, G.H. Chen, Potent antibacterial activities of Ag/TiO_2 nanocomposite powders synthesized by a one-pot sol–gel method, Environ. Sci. Technol. 43 (2009) 2905–2910.
[22] D. Lutzenkirchen-Hecht, H.H. Strehblow, Anodic silver (II) oxides investigated by combined electrochemistry, *ex situ* XPS and *in situ* X-ray absorption spectroscopy, Surf. Interface Anal. 41 (2009) 820–829.
[23] A. Mekki, XPS study of lead vanadate glasses, Arab J. Sci. Eng. 28 (2003) 73–85.
[24] V. Dimitrov, T. Komatsu, Classification of simple oxides: a polarizability approach, J. Solid State Chem. 163 (2002) 100–112.
[25] F.E. Lopez-Suarez, A. Bueno-Lopez, M.J. Illan-Gomez, A. Adamski, B. Ura, J. Trawczynski, Copper catalysts for soot oxidation: alumina versus perovskite supports, Environ. Sci. Technol. 42 (2008) 7670–7675.
[26] H. He, H.X. Dai, C.T. Au, An investigation on the utilization of perovskite-type oxides $La_{1-x}Sr_xMO_3$ (M = $Co_{0.77}Bi_{0.20}Pd_{0.03}$) as three-way catalysts, Appl. Catal. B: Environ. 33 (2001) 65–80.
[27] Y. Hu, U.L. Lin, N.H. Liu, Effect of copper valence on the glass structure and crystallization behavior of Bi–Pb–Cu–O glasses, Mater. Chem. Phys. 49 (1997) 115–119.
[28] H. Mizoguchi, P.M. Woodward, Electronic structure studies of main group oxides possessing edge-sharing octahedra: implications for the design of transparent conducting oxides, Chem. Mater. 16 (2004) 5233–5248.
[29] L.H. Chia, X.M. Tang, L.K. Weavers, Kinetics and mechanism of photoactivated periodate reaction with 4-chlorophenol in acidic solution, Environ. Sci. Technol. 38 (2004) 6875–6880.
[30] S.T. Martin, A.T. Lee, M.R. Hoffmann, Chemical mechanism of inorganic oxidants in the TiO_2/UV process: increased rates of degradation of chlorinated hydrocarbons, Environ. Sci. Technol. 29 (1995) 2567–2573.
[31] L. Wu, A.M. Li, G.D. Gao, Z.H. Fei, S.R. Xu, Q.X. Zhang, Efficient photodegradation of 2,4-dichlorophenol in aqueous solution catalyzed by polydivinylbenzene-supported zinc phthalocyanine, J. Mol. Catal. A: Chem. 169 (2007) 183–189.
[32] E. Benhur, A. Carmichael, P. Riesz, I. Rosenthal, Photochemical generation of superoxide radical and the cyto-toxicity of phthalocyanines, Int. J. Radiat. Biol. 48 (1985) 837–846.
[33] A.Y. Shvykin, V.V. Platonov, V.P. Proskuryakov, K.B. Chilachava, E.M. Khmarin, I.V. Kovtun, Bismuth (V) oxide and silver bismuthate as oxidizing agents for gas-chromatographic elemental microanalysis, Russ. J. Appl. Chem. 77 (2004) 1200–1202.
[34] J.W. Peters, P.J. Bekowies, A.M. Winer, J.N. Pitts Jr., Potassium perchromate as a source of singlet oxygen, J. Am. Chem. Soc. 97 (1975) 3299–3306.